Available online at www.sciencedirect.com

ScienceDirect

IFAC PapersOnline CONFERENCE PAPER ARCHIVE

IFAC PapersOnLine 53-2 (2020) 14285–14291

Optimal Sliding Mode Control Method for Active Suspension Control

Kerem Bayar* Farshid-Sadeghi Khaneghah**

**Middle East Technical University, Mechanical Engineering Department Ankara, Turkey (Tel: +90 5377676686; e-mail: kbayar@metu.edu.tr).*
***Middle East Technical University, Mechanical Engineering Department Ankara, Turkey (Tel: +905522404791; e-mail: farshid.khaneghah@metu.edu.tr).*

Abstract: A non-linear quarter car vehicle model is used in this study, for developing an active suspension control algorithm. The control method used is optimal sliding mode control, along with feedback linearization technique for compensating the nonlinear aspects of the plant. In addition to the work in recent literature that applies these control methods, estimation of the static suspension deflection; i.e. vehicle sprung mass is performed. Through simulation results, it is shown that correct information of vehicle sprung mass, compared to taking it as a constant parameter in control design, improves the performance of the controller. This in turn, reduces the sprung mass acceleration level, and enhances ride comfort.

Keywords: Active suspension, optimal sliding mode control, feedback linearization, extended Kalman filter

1. INTRODUCTION

Ride comfort is among the most important assessment criteria regarding automobiles and buses today. The current trend is usage of semi-active [Savaresi et al. 2010] and active suspension systems [Liu et al. 2014] for improving ride comfort.

Active suspension systems have a separate actuator, that can add or subtract force, independent of the passive components. In that sense, they are superior to semi-active ones [Gysen et al. 2008].

Different control methods are applied for active suspension control purpose. Among these are H_∞ control [Wang et al. 2015], backstepping [Savaş ve Baştürk 2017, Schwarzgruber et al. 2010] and sliding mode control [Pan et al. 2015]. A special version of sliding mode control on the other hand, named as "optimal sliding mode control" [Utkin 1992] is very suitable for active suspension control purpose. The reason of this is that the Eigenvalues of the desired sliding mode motion is specified with respect to a cost function. This cost function constitutes of weighted wheel travel, suspension deflection and sprung mass acceleration, just like the classical linear quadratic regulator design. By means, not only a control method that is known to be robust against parameter variations and unpredicted disturbances is applied but also the weightings can be tuned according to the priority of the active suspension.

There is a recent study by [Chen et al. 2017] that applies this technique, along with feedback linearization, for active suspension control. In this study, considering a quarter car model that is commonly used for suspension control studies, five states are fed back within a sliding mode control scheme. These are wheel travel, suspension deflection, unsprung and sprung mass speeds, and the fifth state is sprung mass acceleration. The last state is added to the controller in a very similar design scheme to the integrator backstepping with cascade connection [Khalil 2002]. It is reported in this study that the controller performed well in reducing the sprung mass acceleration (which is essential for ride comfort), under varying sprung mass conditions and tire stiffness values, for different road profiles.

In this work, another source of improvement is analyzed, which is knowing the sprung mass correctly for control development purpose. If the initial suspension deflection, which is a direct representation of sprung mass is not known correctly, then there will be three sources of error in determining the required control action. The first one is obviously due to the Kalman filter, which will use a wrong value for the sprung mass. This would cause inaccuracies in state estimation, which in turn would reflect on computation of the required closed loop control action. Second one is the linearizing feedback, which will be given by Equation 7 in Section 3 of this work. Again incorrect vehicle mass (or static suspension deflection) information would cause feedback linearization method to malfunction, which is already vulnerable against usage of estimated states. Lastly the coefficients of the sliding surface, i.e. the desired Eigenvalues of the sliding mode motion would be determined with respect to an incorrect transformation matrix; Equation 15 in Section 3. All these errors in computing the control action would deteriorate the controller performance, which may end up with an increase in sprung mass acceleration. All these items are discussed and detailed in the third section with simulation results, considering two different vehicle mass scenarios, after describing the system and writing the non-linear state space and extended Kalman filter equations in the next section.

2. QUARTER CAR MODEL WITH NON-LINEAR STATE EQUATIONS

Quarter car model, that is illustrated in Figure 1, is commonly applied in semi-active and active suspension control studies [Chen et al. 2016]. Representing the suspension deflection vs

10.1016/j.ifacol.2020.12.1178

suspension spring force characteristics in a non-linear fashion is more realistic. Also the suspension damper force exhibits a non-linear force characteristic; the damping coefficient is typically higher during rebound phase compared to bump phase [Dixon 2007], as shown in Figure 2.

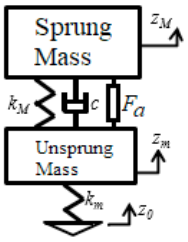

Figure 1. Quarter car model used for suspension control algorithm development

Equation 1 gives the differential equations of motion for the quarter car model shown in Figure 1.

$$\begin{aligned} M\,\ddot{z}_M &= k_{s1}\left(z_m - z_M - d_{so}\right) + k_{s2}\left(z_m - z_M - d_{so}\right)^3 + c\left(\dot{z}_m - \dot{z}_M\right) \\ &\quad - Mg + F_a \\ m\,\ddot{z}_m &= -k_{s1}\left(z_m - z_M - d_{so}\right) - k_{s2}\left(z_m - z_M - d_{so}\right)^3 - c\left(\dot{z}_m - \dot{z}_M\right) - F_a \\ &\quad - mg + k_t\left(z_0 - z_m - d_{to}\right) \end{aligned} \tag{1}$$

where M and m represent one quarter of the sprung mass of the vehicle and the unsprung mass associated with a single wheel respectively, k_{s1} and k_{s2} are the spring stiffness for the linear and the non-linear portion of the spring force, k_t is the tire stiffness of the tire, c is the damping coefficient of the damper, g is the gravitational acceleration, d_{so} is the suspension deflection at static equilibrium, and F_a represents the controlled linear motor force. z_0 represents the random road profile, z_m and z_M represent the vertical unsprung, and sprung mass motion, respectively. Here the non-linear spring force characteristic is emphasized. The values for these parameters (except the maximum motor force) were obtained by modifying the ones in [Chen et al. 2017], which are listed in Table 1 below:

Table 1. Quarter car model parameters

Nominal static suspension deflection, d_{so} [m]	-0.15
Nominal quarter sprung mass, M [kg]	1234
Unsprung mass, m [kg]	100
Linear spring stiffness coefficient, k_{s1} [N/m]	80000
Non-linear spring stiffness coefficient, k_{s2} [N/m^3]	32000
Tire stiffness, k_t [N/m]	405000
Max motor force, $\lvert F_a \rvert$ [N]	2703

If one derives the static deflection d_{so} of the sprung mass at stationary condition, and d_{to}; the static tire deflection, then the following expressions may be written relating the static deflections d_{so} and d_{to} with the sprung and unsprung masses:

$$\begin{aligned} k_{1s} d_{so} + k_{2s} d_{so}^3 &= -Mg \\ k_t d_{to} &= -\left(m + M\right) g \end{aligned} \tag{2}$$

For the damping coefficient c, the following expression is used to represent typical asymmetrical characteristic of the damper force with respect to damper speed in the bump and rebound conditions, illustrated in Figure 2.

$$c = 775\text{atan}\left(50\left(\dot{z}_s - \dot{z}_u\right)\right) + 2800 \tag{3}$$

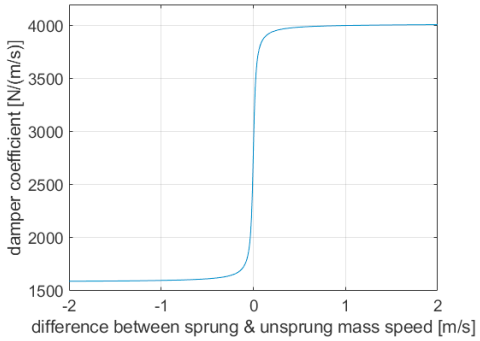

Figure 2. Typical asymmetrical damper force characteristic.

Arctangent function is used here to approximate the sign function with a differentiable function for controller development purposes, such as checking the rank of the controllability & observability matrices, as explained in [Hedrick and Girard 2015].

If Equations 2 & 3 are substituted into Equation set (1) for eliminating M from the equations, then one may obtain the following expressions for the sprung mass acceleration and the unsprung mass accelerations, respectively.

$$\begin{aligned} \ddot{z}_m &= \frac{k_t\left(z_0 - z_m\right) - k_{1s}\left(z_m - z_M\right) - k_{2s}\left[\left(z_m - z_M\right)^3 - 3\left(z_m - z_M\right)^2 d_{so} + 3\left(z_m - z_M\right) d_{so}^2\right]}{m_u} \\ &\quad - \frac{\left(775\text{atan}\left(50\left(\dot{z}_s - \dot{z}_u\right)\right) + 2800\right)\left(\dot{z}_m - \dot{z}_M\right)}{m_u} - \frac{1}{m_u} F_a \\ \ddot{z}_M &= \frac{g\left[k_{1s}\left(z_m - z_M\right) + k_{2s}\left[\left(z_m - z_M\right)^3 - 3\left(z_m - z_M\right)^2 d_{so} + 3\left(z_m - z_M\right) d_{so}^2\right]\right]}{-k_{1s} d_{so} - k_{2s} d_{so}^3} \\ &\quad + \frac{g\left(775\text{atan}\left(50\left(\dot{z}_s - \dot{z}_u\right)\right) + 2800\right)\left(\dot{z}_m - \dot{z}_M\right)}{-k_{1s} d_{so} - k_{2s} d_{so}^3} + \frac{g}{-k_{1s} d_{so} - k_{2s} d_{so}^3} F_a \end{aligned} \tag{4}$$

To write the state space equations, the following state choices should be made, that is commonly applied for suspension control purposes:

$$\begin{aligned} x_1 &= z_0 - z_m \\ x_2 &= z_m - z_M \\ x_3 &= \dot{z}_m \\ x_4 &= \dot{z}_M \end{aligned} \tag{5}$$

So the states are taken as, tire deflection, suspension deflection, unsprung and sprung mass speeds.

The two measurements on the other hand are the two acceleration measurements; unsprung and sprung mass accelerations. An accelerometer measuring the sprung mass acceleration is already a standard in many production vehicles. The accelerometer for the unsprung mass is the additional hardware in this proposed active suspension control system.

With the states defined above, the non-linear state and output equations can be formulated as:

$$\begin{Bmatrix}\dot{x}_1\\ \dot{x}_2\\ \dot{x}_3\\ \dot{x}_4\end{Bmatrix}=\begin{Bmatrix}-x_3\\ x_3-x_4\\ \dfrac{k_t x_1-k_{1s}x_2-k_{2s}\left(x_2^3-3x_2^2d_{so}+3x_2d_{so}^2\right)-\left(775\text{atan}\left(50\left(x_4-x_3\right)\right)+2800\right)\left(x_3-x_4\right)}{m_u}\\ \dfrac{g\left[k_{1s}x_2+k_{2s}\left[x_2^3-3x_2^2d_{so}+3x_2d_{so}^2\right]+\left(775\text{atan}\left(50\left(x_4-x_3\right)\right)+2800\right)\left(x_3-x_4\right)\right]}{-k_{1s}d_{so}-k_{2s}d_{so}^3}\end{Bmatrix}$$
$$+\begin{bmatrix}0\\0\\-\dfrac{1}{m_u}\\ \dfrac{g}{-k_{1s}d_{so}-k_{2s}d_{so}^3}\end{bmatrix}F_a+\begin{bmatrix}1\\0\\0\\0\end{bmatrix}\dot{z}_0$$
$$\begin{Bmatrix}h_1(x)\\ h_2(x)\end{Bmatrix}=\begin{Bmatrix}\dfrac{k_t x_1-k_{1s}x_2-k_{2s}\left(x_2^3-3x_2^2d_{so}+3x_2d_{so}^2\right)-\left(775\text{atan}\left(50\left(x_4-x_3\right)\right)+2800\right)\left(x_3-x_4\right)}{m_u}\\ \dfrac{g\left[k_{1s}x_2+k_{2s}\left[x_2^3-3x_2^2d_{so}+3x_2d_{so}^2\right]+\left(775\text{atan}\left(50\left(x_4-x_3\right)\right)+2800\right)\left(x_3-x_4\right)\right]}{-k_{1s}d_{so}-k_{2s}d_{so}^3}\end{Bmatrix}$$
$$+\begin{bmatrix}-\dfrac{1}{m_u}\\ \dfrac{g}{-k_{1s}d_{so}-k_{2s}d_{so}^3}\end{bmatrix}F_a+\begin{bmatrix}1&0\\0&1\end{bmatrix}\begin{Bmatrix}v_1\\v_2\end{Bmatrix} \tag{6}$$

where v_1 and v_2 represent zero mean white noise processes, associated with accelerometer noise, with covariance R_1 and R_2, respectively. The time derivative of the road profile, $\dot{z}_0$, on the other hand, is treated as the process error with covariance Q in writing the extended Kalman filter equations in the next section. The parameters used for simulation purpose, and in the extended Kalman filter algorithm are listed in Table 2.

Table 2. Controller parameters

Controller sampling rate, τ [milli-second]	1
Accelerometer noise covariance; R_1 and R_2 [m/s^2]^2	0.5
Road profile speed covariance, Q [m/s]^2	0.0111
Static suspension deflection, process noise covariance [m]^2	6.25.10^{-4}

3. PROPOSED CONTROLLER

In this study, by applying the feedback linearization technique [Isidori 1995] to avoid the non-linearities in the state equations, a sliding mode controller [Utkin et al. 2009] of the following form is structured:

$$F_a=\frac{-k_{1s}\left(d_{so}\right)_{est}-k_{2s}\left(d_{so}\right)_{est}^3}{g}\left\{-K\tanh\left[3\left(K_{a1}\hat{x}_1+K_{a2}\hat{x}_2+K_{a3}\hat{x}_3+K_{a4}\hat{x}_4\right)\right]\right\}$$
$$-k_{1s}\hat{x}_2-k_{2s}\left(\hat{x}_2^3-3\hat{x}_2^2\left(d_{so}\right)_{est}+3\hat{x}_2\left(d_{so}\right)_{est}^2\right)$$
$$-\left(775\text{atan}\left[50\left(\hat{x}_4-\hat{x}_3\right)\right]+2800\right)\left(\hat{x}_3-\hat{x}_4\right) \tag{7}$$

where $(d_{so})_{est}$ is the estimated suspension static deflection, and $\hat{x}_1,\hat{x}_2,\hat{x}_3,\hat{x}_4$ represent the estimated states. tanh function is used to approximate the sign function of the sliding mode controller, to avoid chattering.

Note that the input F_a affects the output directly, as seen in Equation set 6. By means, the relative degree of the system is not defined in the usual way (it can be assumed to be zero), and the expression given by Equation 7 becomes sufficient to linearize the system. The reader is referred to [Chen et al. 2017] for the details of this derivation. There are two differences of this work, compared to the referred study: The first one is that the sliding mode controller uses four states, as seen in Equation set 6 and Equation 7, instead of adding the sprung mass acceleration as the fifth one. The second difference is related to the main claim in this paper, as mentioned in the Introduction section as well: Correct knowledge of d_{so} would improve the effectiveness of the sliding mode control. There are three reasons of this: 1) In the extended Kalman filter equations that will be introduced next, for estimating the four states correctly, correct information of d_{so} is needed, otherwise there will be an estimation error. This would further degrade the performance of the feedback linearization method, which is already vulnerable against feedback of estimated states for linearization purpose. 2) The linearizing term, given by Equation 7 above, will eliminate the nonlinearities in the fourth state equation in Equation set 6, only if the estimated d_{so} equals the actual d_{so}. Otherwise, under conditions where it is taken as a constant, and no estimation is done, the error will cause increases in sprung mass acceleration. 3) Due to wrong d_{so} information, the desired Eigenvalues of the sliding mode motion will deviate from the optimal ones, that are determined by the cost function. This will be another source of increase in sprung mass acceleration. The Kalman filer is introduced next, and the last two aforementioned item will be detailed.

3.1 Extended Kalman Filter & Controller

There are two extended Kalman filters utilized in the controller: The first one is basically responsible for estimating d_{so}, with the controller off. This is to eliminate the errors explained above, which will later be quantified by simulation results in this section. In addition to the four states given by Equation set 6, a fifth state, d_{so}, is introduced. With this, the state and output equations with no control action can be expressed as:

$$\begin{Bmatrix}\dot{x}_1\\ \dot{x}_2\\ \dot{x}_3\\ \dot{x}_4\\ \dot{x}_5\end{Bmatrix}=\begin{Bmatrix}-x_3\\ x_3-x_4\\ \dfrac{k_t x_1-k_{1s}x_2-k_{2s}\left(x_2^3-3x_2^2x_5+3x_2x_5^2\right)-\left(775a\tan\left(50\left(x_4-x_3\right)\right)+2800\right)\left(x_3-x_4\right)}{m_u}\\ \dfrac{g\left[k_{1s}x_2+k_{2s}\left[x_2^3-3x_2^2x_5+3x_2x_5^2\right]+\left(775a\tan\left(50\left(x_4-x_3\right)\right)+2800\right)\left(x_3-x_4\right)\right]}{-k_{1s}x_5-k_{2s}x_5^3}\\ 0\end{Bmatrix}$$
$$+\begin{bmatrix}1&0\\0&0\\0&0\\0&0\\0&1\end{bmatrix}\begin{bmatrix}\dot{z}_0\\ w\end{bmatrix}$$
$$\begin{Bmatrix}h_1(x)\\ h_2(x)\end{Bmatrix}=\begin{Bmatrix}\dfrac{k_t x_1-k_{1s}x_2-k_{2s}\left(x_2^3-3x_2^2x_5+3x_2x_5^2\right)-\left(775a\tan\left(50\left(x_4-x_3\right)\right)+2800\right)\left(x_3-x_4\right)}{m_u}\\ \dfrac{g\left[k_{1s}x_2+k_{2s}\left[x_2^3-3x_2^2x_5+3x_2x_5^2\right]+\left(775a\tan\left(50\left(x_4-x_3\right)\right)+2800\right)\left(x_3-x_4\right)\right]}{-k_{1s}x_5-k_{2s}x_5^3}\end{Bmatrix}$$
$$+\begin{bmatrix}1&0\\0&1\end{bmatrix}\begin{Bmatrix}v_1\\v_2\end{Bmatrix} \tag{8}$$

The equations for the extended Kalman filter can be summarized as follows, which gives the Kalman gain, state estimation covariance, state update, state prediction and posteriori covariance, respectively.

$$K_k = P_{k/k-1}\left[\frac{\partial h}{\partial x}\left(\hat{x}_{k/k-1}\right)\right]^T\left\{\left[\frac{\partial h}{\partial x}\left(\hat{x}_{k/k-1}\right)\right]P_{k/k-1}\left[\frac{\partial h}{\partial x}\left(\hat{x}_{k/k-1}\right)\right]^T + R\right\}^{-1}$$

$$P_{k/k} = P_{k/k-1} - K_k\left[\frac{\partial h}{\partial x}\left(\hat{x}_{k/k-1}\right)\right]P_{k/k-1}$$

$$\hat{x}_{k/k} = \hat{x}_{k/k-1} + K_k\left(y - h\left(\hat{x}_{k/k-1}\right)\right)$$

$$\hat{x}_{k+1/k} = f\left(\hat{x}_{k/k}\right)$$

$$P_{k+1/k} = \phi\left(\hat{x}_{k/k}\right)P_{k/k}\phi\left(\hat{x}_{k/k}\right) + WQW^T \tag{9}$$

To initialize the extended Kalman filter, three-point initialization method is used [Bar-Shalom et al. 2001]. The d_{so} estimation process with this 5 state extended Kalman filter is concluded, by checking three variables: P_{55}; the state estimation covariance associated with d_{so}, its derivative $(P_{55}-P_{55z})/\tau$ and the derivative of the state estimate itself, $(\hat{x}_5-\hat{x}_{5z})/\tau$. Once these variables fit within pre-specified thresholds, correct d_{so} information is obtained and the extended Kalman filter is deactivated. This procedure is explained by Figure 3, shown below. This figure shows a simulation result, where both d_{so} estimation covariance P_{55}, and the derivative of the estimate itself dropped below pre-specified thresholds, which is highlighted in the figure. Table 3 shows some simulation results for this estimation technique, comparing the actual and the estimated d_{so}.

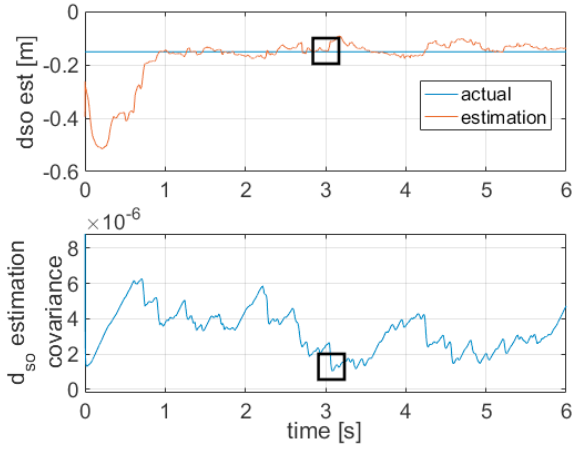

Figure 3. Simulation result for d_{so} estimation, where the real value is 0.15 m. The estimation, based on pre-specified thresholds, is concluded as -0.1495 m, at around three seconds after initialization of the algorithm.

Table 3. Five state Kalman filter, d_{so} estimation results

Actual d_{so} [m]	Estimated d_{so} [m]
-0.15	-0.1495
-0.175	-0.1766
-0.2	-0.2084

It should be stated at this point that, in order to increase the robustness of this estimation algorithm, numerous simulations (not just three cases) should be carried out considering a range of realistic d_{so} values. In each of these simulations, the aforementioned thresholds should be fine-tuned such that these thresholds are affective in estimating all d_{so} values correctly, in this range.

Once d_{so} estimation is finished, the order of the state space is reduced back to four states taking Equation set 6 into account, this time with the controller on. So the extended Kalman filter equations become:

$$K_k = P_{k/k-1}\left[\frac{\partial h}{\partial x}\left(\hat{x}_{k/k-1}\right)\right]^T\left\{\left[\frac{\partial h}{\partial x}\left(\hat{x}_{k/k-1}\right)\right]P_{k/k-1}\left[\frac{\partial h}{\partial x}\left(\hat{x}_{k/k-1}\right)\right]^T + R\right\}^{-1}$$

$$P_{k/k} = P_{k/k-1} - K_k\left[\frac{\partial h}{\partial x}\left(\hat{x}_{k/k-1}\right)\right]P_{k/k-1}$$

$$\hat{x}_{k/k} = \hat{x}_{k/k-1} + K_k\left(y - h\left(\hat{x}_{k/k-1}\right) - D\left(F_a\right)_{k-1}\right)$$

$$\hat{x}_{k+1/k} = f\left(\hat{x}_{k/k}\right) + B\left(F_a\right)_k$$

$$P_{k+1/k} = \phi\left(\hat{x}_{k/k}\right)P_{k/k}\phi\left(\hat{x}_{k/k}\right) + WQW^T \tag{10}$$

with d_{so} treated as a constant now, instead of the fifth state, and the control input F_a shows up in the third and the fourth equations in Equation set 10 above, multiplied by the control gain matrices D and B, respectively, as given in Equation set 6.

With the controller expression Equation 7, substituted into Equation set 6, and considering that the state estimation errors are negligible, the fourth equation; i.e. sprung mass acceleration equation becomes:

$$\dot{x}_4 = \frac{gk_{2s}\left(3x_2^2\left(d_{soest} - d_{so}\right) + 3x_2\left(d_{so}^2 - d_{soest}^2\right)\right)}{-k_{1s}d_{so} - k_{2s}d_{so}^3}$$

$$+\frac{k_{1s}d_{soest} + k_{2s}d_{soest}^3}{k_{1s}d_{so} + k_{2s}d_{so}^3}\left[-K\tanh\left(K_{a1}x_1 + K_{a2}x_2 + K_{a3}x_3 + K_{a4}x_4\right)\right] \tag{11}$$

When $|d_{soest}| > |d_{so}|$, i.e. when it is estimated wrong, or when it is taken as a constant as in [Chen et al. 2017], but the vehicle mass changes from the initial condition (very likely to happen for a vehicle in a real scenario) then, three things happen, as mentioned before: The d_{so} used in the Kalman filter equations causes incorrect state estimation. Secondly, the sliding mode controller gain K in Equation 11 above will increase in an undesired way; specifically, by 34% considering d_{so} = -0.15 m but the estimated one (or the constant value used in the controller) being -0.2 m, as an example. Lastly, the optimal sliding mode controller, specifies the sliding surface coefficients in such a way that the Eigenvalues associated with the desired sliding mode motion are set incorrectly. Below is a numerical example:

First, with the assumption that $d_{so} = d_{soest}$, when the control input F_a given in Equation 7 is substituted into the Equation set 6, the state space equations are simplified to:

$$\begin{Bmatrix}\dot{x}_1\\ \dot{x}_2\\ \dot{x}_3\\ \dot{x}_4\end{Bmatrix}=\begin{bmatrix}0 & 0 & -1 & 0\\ 0 & 0 & 1 & -1\\ \frac{k_t}{m_u} & 0 & 0 & 0\\ 0 & 0 & 0 & 0\end{bmatrix}\begin{Bmatrix}x_1\\ x_2\\ x_3\\ x_4\end{Bmatrix}+\begin{bmatrix}0\\ 0\\ \frac{k_{1s}d_{so}+k_{2s}d_{so}^3}{m_u g}\\ 1\end{bmatrix}u_a+\begin{bmatrix}1\\ 0\\ 0\\ 0\end{bmatrix}\dot{z}_0 \tag{12}$$

where $u_a = -K \tanh [3(K_{a1}x_1+K_{a2}x_2+K_{a3}x_3+K_{a4}x_4)]$. When the weighting factors of the three important suspension parameters, namely the first state wheel travel, second state suspension deflection and the fourth state sprung mass speed are taken as (the values are modified from [Chen et al. 2017])

$$Q=\begin{bmatrix}\delta_1 & 0 & 0 & 0\\ 0 & \delta_2 & 0 & 0\\ 0 & 0 & 0 & 0\\ 0 & 0 & 0 & \delta_3\end{bmatrix} \tag{13}$$

$$\begin{aligned}&\delta_1 = 35689;\\ &\delta_2 = 27862;\\ &\delta_3 = 10000;\end{aligned} \tag{14}$$

Then the sliding surface coefficients, are computed by using the following transformation matrix M

$$M=\begin{bmatrix}1 & 0 & 0 & 0\\ 0 & 1 & 0 & 0\\ 0 & 0 & 1 & \frac{-k_{1s}d_{so}-k_{2s}d_{so}^3}{m_u g}\\ 0 & 0 & 0 & 1\end{bmatrix} \tag{15}$$

$$A_M = MAM^{-1}=\begin{bmatrix}0 & 0 & -1 & \frac{-k_{1s}d_{so}-k_{2s}d_{so}^3}{m_u g}\\ 0 & 0 & 1 & \frac{k_{1s}d_{so}+k_{2s}d_{so}^3}{m_u g}-1\\ \frac{k_t}{m_u} & 0 & 0 & 0\\ 0 & 0 & 0 & 0\end{bmatrix} \tag{16}$$

$$Q_M = \left(M^{-1}\right)^T QM^{-1}=\begin{bmatrix}\delta_1 & 0 & 0 & 0\\ 0 & \delta_2 & 0 & 0\\ 0 & 0 & 0 & 0\\ 0 & 0 & 0 & \delta_3\end{bmatrix}$$

with

$$A_{M11}=\begin{bmatrix}0 & 0 & -1\\ 0 & 0 & 1\\ \frac{k_t}{m_u} & 0 & 0\end{bmatrix} \qquad A_{M12}=\begin{bmatrix}\frac{-k_{1s}d_{so}-k_{2s}d_{so}^3}{m_u g}\\ \frac{k_{1s}d_{so}+k_{2s}d_{so}^3}{m_u g}-1\\ 0\end{bmatrix} \tag{17}$$

$$Q_{M12}=\begin{bmatrix}0\\ 0\\ 0\end{bmatrix} \qquad Q_{M22}=\delta_3 \tag{18}$$

And with P being the unique solution of the matrix Riccati equation as follows:

$$(PA_{M11})^T+PA_{M11}+Q_{M11}-(PA_{M12}+Q_{M12})Q_{M22}^{-1}(PA_{M12}+Q_{M12})^T = 0 \tag{19}$$

The coefficients of the sliding surface can be derived as:

$$K_a = [Q_{M22}^{-1}(A_{M12}^T P + Q_{M12}^T) \quad I]M \tag{20}$$

when the d_{so} is estimated correct, as -0.15, these values are computed as K_a = [0.8516 -1.6692 0.0004 1.0043], and this sliding surface corresponds to the following desired Eigenvalues of sliding mode motion:

$$\begin{aligned}&-1.6837\\ &-15.5495+61.4277i\\ &-15.5495 -61.4277i\end{aligned} \tag{21}$$

Considering the weighting of the sprung mass speed is reduced to half of its value, namely δ_3 = 5000, then the Eigenvalues become:

$$\begin{aligned}&-2.4025\\ &-21.9787+59.1292i\\ &-21.9787 - 59.1292i\end{aligned} \tag{22}$$

In other words, they increase.

There is a similar effect when the d_{so} is estimated incorrect, for instance -0.2 m. When d_{so} = -0.2, then the transformation matrix M is computed accordingly, and this ends up with the following controller gain K_a = [0.8516 -1.6692 0.0003 1.0058] and the corresponding desired Eigenvalues of sliding mode motion:

$$\begin{aligned}&-1.6888\\ &-20.8764+59.7257i\\ &-20.8764 -59.7257i\end{aligned} \tag{23}$$

In other words, miss-estimating d_{so} makes an effect as if the weighting of the sprung mass speed is reduced. This undesired outcome contributes to the increase in sprung mass speed decay rate, as well. This is the last source of increase in sprung mass acceleration. Table 4 shows simulation results illustrating how much sprung mass acceleration increase is observed due to the aforementioned affects because of incorrect d_{so} information that is used in the control algorithm. The tabulated acceleration is "ISO 2631 filtered" [ISO 1997]; a filter that is derived through experiments to express the effect of vertical vibrations on human body. The road profile used for the simulations is illustrated in Figure 4.

The undesired increase in sprung mass acceleration is evident; from 0.3619 m/s2 to 0.4101 m/s2; i.e. 13%, due to estimating (or taking) it as -0.2084 m whereas the real value is -0.15 m. On the other hand, the increase is 4%, from 0.3379 m/s2 to

0.3501 m/s2, for incorrect knowledge of -0.2 m whereas the real value is -0.175 m.

Table 4. Simulation results comparing correct and incorrect d_{so} information

Actual d_{so} [m]	Estimated d_{so} [m]	ISO 2631 filtered RMS sprung mass acc. [m/s^2]
-0.15	-0.1495	0.3619
-0.15	-0.175	0.3857
-0.15	-0.2084	0.4101
-0.175	-0.1766	0.3379
-0.175	-0.2	0.3501

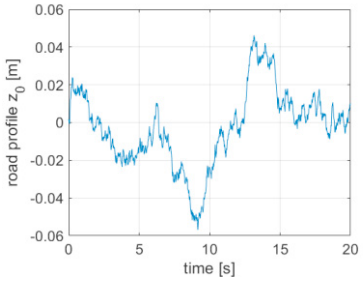

Figure 4. Road profile input z_0 as a function of time.

In regard to these results, it may be concluded that taking a low value for d_{so} within the control algorithm (regardless of the real value) would yield a lower sprung mass acceleration. However, in such a case, the sliding surface coefficients; i.e. the desired Eigenvalues are computed incorrect, again. Table 5 shows the effect of taking a lower d_{so} value within the control algorithm, on the Eigenvalues.

Again, with wrong d_{so} information, shown by the third case of Table 5 (shown by Equation 21 as well), the Eigenvalues reduce compared to the first case where the d_{so} information is correct. There is a similar effect on the Eigenvalues when the weighting of the suspension deflection, δ_2, is reduced, as shown by the second case of Table 5. Therefore, it may be concluded that using a lower d_{so} in the control algorithm, compared to the actual one, would generate a tendency towards undesired suspension deflection increase. This prediction has been checked with simulations. The RMS value for the suspension deflection increased by 13%, when the actual d_{so} is -0.2 m but the one used in the controller is -0.15 m, despite a reduction in sprung mass acceleration.

4. CONCLUSIONS

A potential improvement in the performance of the optimal sliding mode controller explained in [Chen et al. 2017] is given in this work. The improvement is due to real time estimation of the suspension static deflection, i.e. sprung mass. Through simulation results, it was shown that the optimal sliding mode controller would perform better with the correct sprung mass information. This improvement corresponds to 13% and 4% lower ISO 2631 filtered sprung mass acceleration, considering d_{so} = -0.15 m and d_{so} = -0.175 m, respectively.

Table 5. Effect of using a lower d_{so} (actual one is -0.2 m) on the Eigenvalues of the desired sliding mode motion, for different weightings used within the optimal sliding mode controller

	Eigenvalues
δ_1 = 35689; δ_2 = 27862; $(d_{so})_{est}$ = -0.2; δ_3 = 10000;	-1.6888 -20.8764 ± 59.7257
δ_1 = 35689; δ_2 = 27862/2; $(d_{so})_{est}$ = -0.2; δ_3 = 10000;	-1.1872 -18.4521 ± 60.7136i
δ_1 = 35689; δ_2 = 27862; $(d_{so})_{est}$ = -0.15; δ_3 = 10000;	-1.6837 -15.5495 ± 61.4277i

5. ACKNOWLEDGEMENT

This study was conducted under The Scientific and Technological Research Council of Turkey (Tübitak) project number 218M917. Special thanks to Prof. Dr. Umut Orguner of Electrical and Electronics Engineering Department, Middle East Technical University, Ankara, Turkey for guidance on extended Kalman filter initialization.

REFERENCES

Bar-Shalom, Y., Li, X.-R. and Kirubarajan, T. 2001 "Estimation with Applications to Tracking and Navigation" John Wiley & Sons, Inc. ISBN: 0-471-41655-X.

Chen, W., Xiao, H., Wang, Q., Zhao, L. and Zhu, M. 2016 "Integrated Vehicle Dynamics and Control", Wiley. ISBN: 9781118379998.

Chen, S.-A., Wang, J.-C., Yao, M. and Kim, Y.-B. 2017 "Improved Optimal Sliding Mode Control for a Non-linear Vehicle Active Suspension System" Journal of Sound and Vibration, DOI: http://dx.doi.org/10.1016/j.jsv.2017.02.017.

Dixon, J. C. 2007 "The Shock Absorber Handbook", 2nd Edition, ISBN: 978-0-470-51020-9 John Wiley & Sons, Ltd.

Gysen B. L., Janssen J. L., Paulides J. J., and Lomonova E. A. 2008 "Design aspects of an active electromagnetic suspension system for automotive applications" IEEE transactions on Industry Applications, 45, 5, 1589-1597.

Hedrick, J. K. and Girard, A. 2015 "Control of Nonlinear Dynamic Systems: Theory and Applications", available at: https://www.researchgate.net/publication/290128700_Control_of_nonlinear_dynamic_systems_theory_and_applications

Isidori, A 1995 "Nonlinear Control Systems: An Introduction" Springer, ISBN: 978-1-84628-615-5.

ISO 2631 – 1, 1997 "Mechanical vibration and shock – Evaluation of human exposure to whole-body vibration – Part 1: General requirements"

Khalil, H. K. 2002 "Nonlinear Systems", 3rd Edition. Prentice Hall. ISBN: 0-13-067389-7.

Liu, H., Gao H. and Li, P. 2014 “Handbook of Vehicle Suspension Control Systems” ISBN: 978-1-84919-633-8, © The institution of Engineering and Technology, Michael Faraday House.

Pan, H., Sun, W., Gao, H., and Yu, J. 2015. “Finite-time stabilization for vehicle active suspension systems with hard constraints”, IEEE Transactions on Intelligent Transportation Systems, DOI: 10.1109/TITS.2015.2414657.

Savaresi, S.M., Poussot-Vassal, C., Spelta, C., Sename, O. and Dugard, L. 2010 “Semi-Active Suspension Control Design for Vehicles”, ISBN: 978-0-08-096678-6 Butterworth-Heinemann.

Savaş, Y. and Baştürk, H. I. 2017 “Adaptive Backstepping Control Design for Active Suspension Systems Actuated by Four-way Valve-piston”, American Control Conference, Seattle, USA.

Schwarzgruber, T., Grünbacher, E. and Re, L. 2010 “Performance Oriented Tuning Approach for a Non-linear Controlled Active Suspension System”, 8th IFAC Symposium on Nonlinear Control Systems, University of Bologna, Italy.

Utkin, I. U. 1992 “Sliding Modes in Control and Optimization” Springer-Verlag, ISBN: 3-540-53516-0.

Utkin, V., Guldner, J. and Shi, J. 2009 “Sliding Mode Control in Electro-Mechanical Systems” 2nd Edition CRC Press, Taylor & Francis Group. ISBN: 978-1-4200-6560-2.

Wang, R., Jing, H., Karimi, H. R. and Chen, N. 2015 “Robust Fault Tolerant H_∞ Control of Active Suspension Systems with Finite Frequency Constraint”, Mechanical Systems and Signal Processing, DOI: http://dx.doi.org/10.1016/j.ymssp.2015.01.015